Molecular Packing of Functionalized Fluorinated Lipids in Langmuir Mono layers

ARTICLE *in* LANGMUIR · DECEMBER 2010

Impact Factor: 4.46 · DOI: 10.1021/la103743e · Source: PubMed

Langmuir
Article
pubs.acs.org/Langmuir

Molecular Packing of Functionalized Fluorinated Lipids in Langmuir Monolayers

Michael J. Landsberg,[†] Jeremy L. Ruggles,[‡] Waleed M. Hussein,[‡] Ross P. McGeary,[‡,§] Ian R. Gentle,[‡,⊥] and Ben Hankamer*[,†]

[†]*Institute for Molecular Bioscience,* [‡]*School of Chemistry and Molecular Biosciences, and* [§]*School of Pharmacy, The University of Queensland, St. Lucia, Queensland 4072, Australia.* [⊥] *Present address: Australian Synchrotron, 800 Blackburn Rd, Clayton, Victoria, 3168, Australia*

Received September 18, 2010. Revised Manuscript Received November 3, 2010

Fluorinated amphipaths are a fascinating class of compounds, which, despite significant challenges associated with their syntheses, have found use across a number of areas of biotechnology. Applications range from the *in vitro* stabilization of membrane proteins to the development of enhanced stability intravenous drug and gene delivery systems. More recently, monolayer-forming fluorinated lipids have found use in the 2D crystallization of detergent-solubilized hydrophobic or partially hydrophobic proteins at the air−water interface. In this study, we investigate the surface properties of a novel suite of monolayer forming, partially fluorinated lipids. These modular lipid structures contain a densely fluorinated insertion in the hydrocarbon tail and a synthetically modifiable headgroup. Analyses of surface-pressure area isotherms and X-ray reflectometry profiles reveal that the lipids spread into fluid monolayers and are more compressible than their non-fluorinated counterparts. Furthermore, the data support a model whereby the partially fluorinated chains of the lipid tails form a film which is fundamentally incompatible with detergents and other destabilizing amphipaths.

Introduction

Fluorinated lipids are a fascinating class of compounds rapidly growing in importance. Their synthesis is often challenging as a result of their unusual reactivity and poor solvent compatibility. Despite these challenges, fluorinated lipids and related amphipathic molecules are becoming increasingly important components across a range of biotechnological and biomedical applications. Single-chain fluorinated surfactants hold promise for a number of exciting applications including the stabilization of membrane proteins for *in vitro* studies, either during cell-free expression or following membrane extraction. Fluorinated surfactants substituted for standard detergents have, for example, been shown to reduce denaturation and dissociation of detergent-sensitive proteins and protein complexes.[1−4] Liposome-forming fluorinated lipids, which exhibit reduced permeability, enhanced stability, and enhanced resistance to disruptive biocompounds and bile salts, have been used in the development of new intravenous drug and gene delivery systems.[5,6] More recently, monolayer-forming fluorinated lipids have found use in the 2D crystallization of hydrophobic or partially hydrophobic proteins at the air−water interface.[7]

All of these important developments are underpinned by the unique solution properties of perfluorinated carbon chains. Fluorine is able to functionally substitute for hydrogen, meaning that fluorocarbons, like hydrocarbons, are hydrophobic. Moreover, fluorocarbons have a larger surface area and molecular density when compared to their corresponding hydrocarbons,[8] and as the hydrophobic effect scales proportionally to surface area, fluorocarbons are expected and observed to have enhanced hydrophobicity.[9] Fluorine additionally possesses the highest electronegativity of any element, which in turn results in very low atomic polarizability.[8] This means that fluorocarbon chains exhibit low intermolecular attractive forces and also have a low susceptibility to the formation of temporary multipoles which drive London dispersion forces, the dominant intermolecular interaction in lipophilic compounds. The low susceptibility of fluorocarbons to these forces means that fluorocarbons possess the unusual property of being both hydrophobic and lipophobic.[5] Importantly, fluorocarbons are not readily soluble in water or organic solvents and so tend to form a stable third phase.

Partially fluorinated lipid compounds combine the self-organizational properties of CH_n-based lipids with the unique solution properties of fluorocarbons (CF_n). Fluorinated lipids, like perfluorocarbons, are observed to form a third phase immiscible with aqueous and nonpolar solvents. The incompatibility of the fluorocarbon chains with both hydrophilic and lipophilic structures drives a strong self-association of the fluorinated regions, leading to the formation of a highly stable fluorinated film.[10] As such, partially fluorinated lipid layers appear to be more resistant to permeation and destabilization by a range of small, hydrophobic and/or disruptive molecules.[11−13] Partially fluorinated lipids also appear to be

*To whom correspondence should be addressed. Tel: +61 7 3346 2012. Fax: +61 7 3346 2101. E-mail: b.hankamer@uq.edu.au.

(1) Breyton, C.; Chabaud, E.; Chaudier, Y.; Pucci, B.; Popot, J. L. *FEBS Lett.* **2004**, *564*, 312–318.
(2) Chabaud, E.; Barthelemy, P.; Mora, N.; Popot, J. L.; Pucci, B. *Biochimie* **1998**, *80*, 515–530.
(3) Lebaupain, F.; Salvay, A. G.; Olivier, B.; Durand, G.; Fabiano, A. S.; Michel, N.; Popot, J. L.; Ebel, C.; Breyton, C.; Pucci, B. *Langmuir* **2006**, *22*, 8881–8890.
(4) Park, K. H.; Berrier, C.; Lebaupain, F.; Pucci, B.; Popot, J. L.; Ghazi, A.; Zito, F. *Biochem. J.* **2007**, *403*, 183–187.
(5) Krafft, M. P. *Adv. Drug Delivery Rev.* **2001**, *47*, 209–228.
(6) Vierling, P.; Santaella, C.; Greiner, J. *J. Fluorine Chem.* **2001**, *107*, 337–354.
(7) Hussein, W. M.; Ross, B. P.; Landsberg, M. J.; Hankamer, B.; McGeary, R. P. *Curr. Org. Chem.* **2009**, *13*, 1378–1405.
(8) Lemal, D. M. *J. Org. Chem.* **2004**, *69*, 1–11.
(9) Mukerjee, P. *Colloids Surf., A* **1994**, *84*, 1–10.
(10) Santaella, C.; Vierling, P. *Chem. Phys. Lipids* **1995**, *77*, 173–177.
(11) Held, P.; Lach, F.; Lebeau, L.; Mioskowski, C. *Tetrahedron Lett.* **1997**, *38*, 1937–1940.
(12) Santaella, C.; Frezard, F.; Vierling, P.; Riess, J. G. *FEBS Lett.* **1993**, *336*, 481–484.
(13) McIntosh, T. J.; Simon, S. A.; Vierling, P.; Santaella, C.; Ravily, V. *Biophys. J.* **1996**, *71*, 1853–68.

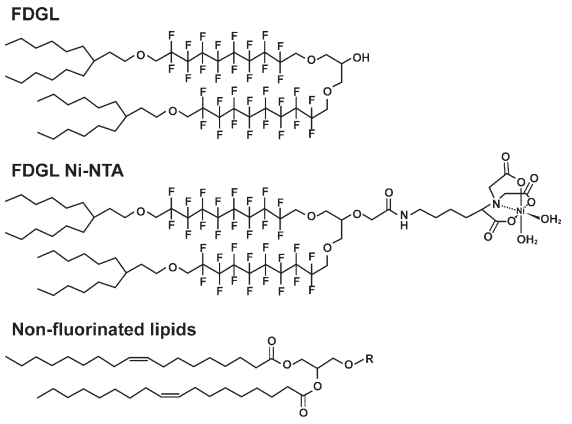

Figure 1. Chemical structures of the fluorinated lipids used in this study FDGL and FDGL-NTA-Ni. FDGL is used as a diluent lipid in forming monolayers for the growth of 2D membrane protein crystals. FDGL Ni-NTA has an additional Ni-chelating headgroup which has a high affinity for polyhistidine tags of recombinant fusion proteins. The non-fluorinated lipids used were DOPC [R = $PO_3^-(CH_2)_2N^+(CH_3)_3$] and DOGS-NTA-Ni [R = $CO(CH_2)_2CO$-$NH(CH_2)_4CH(COO^-)N(CH_2COO^-)Ni^{2+}(OH_2)_2$].

more ordered and significantly more rigid in the fluid phase than their non-fluorinated counterparts.[10]

Subsequently, a number of studies have sought to develop a new class of functionalized, partially fluorinated lipids to facilitate template-assisted 2D crystallization of detergent-solubilized membrane proteins.[14−17] Ni-chelating lipid monolayers have considerable promise for template-assisted 2D crystallization of detergent-solubilized His-tagged membrane proteins, but aside from some notable exceptions,[18−21] the general susceptibility of traditional lipid monolayers to detergent solubilization limits this technology. Recently, we described the synthesis of a novel set of partially fluorinated lipids (Figure 1) for template-assisted 2D crystallization.[16] These lipids were specifically designed to possess the necessary fluidity and detergent resistance for the crystallization of detergent-solubilized membrane proteins at the air−water interface. The perfluorinated region is introduced between the spacer and the branched hydrocarbon tail (Figure 1), a feature different to lipids developed for therapeutic purposes which are usually fluorinated at the end of one or both lipid tails to maximize stability.[6,10,13,22,23] By contrast, insertion of the perfluorinated region in the middle of the monolayer-forming lipids[17] theoretically facilitates the formation of a tightly packed fluorinated film, acting as a spacer between the hydrophilic and hydrophobic parts of the molecule. The branching of the hydrocarbon tails (designed to confer enhanced monolayer fluidity, thereby facilitating lateral diffusion of proteins bound to the functionalized lipid head groups) is more extensive in these lipids compared to those reported previously.[17]

The surface properties of the lipids studied here (Figure 1) are difficult to predict due to both structural differences compared with those characterized previously[13−15,17,24] as well as the limited reported studies of fluorinated lipids in general. Consequently, the focus of this paper is on reporting the properties of Langmuir monolayers formed by these lipids. We show using surface pressure−area isotherms and X-ray reflectometry that these fluorinated lipids spread into stable, fluid monolayers at the air−water interface. In addition, the fluorolipids characterized here have a larger limiting molecular area and a greater electron density in the perfluorinated region of the monolayer than non-fluorinated lipids typically used for protein binding and template-mediated crystallization studies. Implications for template-mediated 2D crystallization of detergent-solubilized proteins are discussed.

Materials and Methods

Lipids. The fluorinated lipids 12,12,13,13,14,14,15,15,16,16,17,17,18,18,19,19,27,27,28,28,29,29,30,30,31,31,32,32,33,33,34,34-dotriacontafluoro-7,39-dihexyl-10,21,25,36-tetraoxapentatetracontan-23-ol (FDGL; Figure 1) and (*S*)-2-(carboxymethyl)-16,16,17,17,18,18,19,19,20,20,21,21,22,22,23,23-hexadecafluoro-12-((2,2,3,3,4,4,5,5,6,6,7,7,8,8,9,9-hexadecafluoro-10-(3-hexylnonyloxy)decyloxy)methyl)-28-hexyl-9-oxo-11,14,25-trioxa-2,8-diazatetratriacontane-1,3-dicarboxylic acid−nickel salt (FDGL-NTA-Ni; Figure 1) were synthesized as described previously.[16] The identities of the compounds were verified by high-resolution mass spectrometry as well as ^1H and ^{13}C NMR spectroscopy, and nickel incorporation into FDGL-NTA-Ni was verified by atomic absorption spectroscopy. 1,2-Dioleoyl-*sn*-glycero-3-phosphocholine and 1,2-dioleoyl-*sn*-glycero-3-[(*N*-(5-amino-1-carboxypentyl)iminodiacetic acid)succinyl] (nickel salt) (DOPC and DOGS-NTA-Ni, respectively) were purchased from Avanti Polar Lipids Inc. (Alabaster, AL) and used without further purification.

Surface Pressure−Area Isotherms. For Langmuir trough experiments, solutions of FDGL, FDGL-NTA-Ni, and 1:1 FDGL/FDGL-NTA-Ni dissolved in 1:1 chloroform/methanol (2.5 mg mL^{-1}) were spread on a pure subphase of Milli-Q water (resistivity >18.2 MΩ cm^{-1}). Comparative experiments were also performed using solutions of DOPC, DOGS-NTA-Ni, and 1:1 DOPC/DOGS-NTA-Ni, prepared at equivalent concentrations. Surface pressure versus area isotherms ($\pi-A$) were measured at 296 K using a surface film balance (model 601S, NIMA Technology, Coventry, England) at a compression rate of 20 cm^2 min^{-1}. Monolayers were allowed to stabilize for at least 20 min before compression commenced. Surface pressure was measured via the Wilhelmy plate method using Whatman 1 Ch paper plates (Whatman International Ltd., Middlesex, England).

X-ray Reflectometry. X-ray reflectometry measurements of the Langmuir monolayers formed by FDGL, FDGL-NTA-Ni, DOPC, and DOGS-NTA-Ni were carried out on the undulator beamline, BL-15-IDC (ChemMatCARS) at the Advanced Photon Source (APS, Argonne National Laboratory, IL) using an X-ray liquid surface reflectometer designed by Schlossman et al.[25] The wavelength of the radiation used was 1.5 Å, and the vertical beam size at the sample was 0.1 mm. $\pi-A$ isotherms and reflectivity profiles were recorded on films spread on subphases in a PTFE trough (NIMA Technologies, Coventry, England), with Wilhelmy plates made from Whatman Ch 1 filter paper. Reflectometry data were collected for all of the films to a maximum Q_z of between 0.40 and 0.60 $Å^{-1}$ (where Q_z is the wave-vector transfer perpendicular to

(14) Courty, S.; Lebeau, L.; Martel, L.; Lenne, P. F.; Balavoine, F.; Dischert, W.; Konovalov, O.; Mioskowski, C.; Legrand, J. F.; Venien-Bryan, C. *Langmuir* **2002**, *18*, 9502–9512.
(15) Dauvergne, J.; Polidori, A.; Venien-Bryan, C.; Pucci, B. *Tetrahedron Lett.* **2008**, *49*, 2247–2250.
(16) Hussein, W. M.; Ross, B. P.; Landsberg, M. J.; Levy, D.; Hankamer, B.; McGeary, R. P. *J. Org. Chem.* **2009**, *74*, 1473–1479.
(17) Lebeau, L.; Lach, F.; Venien-Bryan, C.; Renault, A.; Dietrich, J.; Jahn, T.; Palmgren, M. G.; Kuhlbrandt, W.; Mioskowski, C. *J. Mol. Biol.* **2001**, *308*, 639–647.
(18) Arechaga, I.; Fotiadis, D. *J. Struct. Biol.* **2007**, *160*, 287–94.
(19) Levy, D.; Mosser, G.; Lambert, O.; Moeck, G. S.; Bald, D.; Rigaud, J. L. *J. Struct. Biol.* **1999**, *127*, 44–52.
(20) Plisson, C.; Drucker, M.; Blanc, S.; German-Retana, S.; Le Gall, O.; Thomas, D.; Bron, P. *J. Biol. Chem.* **2003**, *278*, 23753–61.
(21) Fontaine, P.; Faure, M. C.; Muller, F.; Poujade, M.; Micha, J. S.; Rieutord, F.; Goldmann, M. *Langmuir* **2007**, *23*, 12959–65.
(22) Frezard, F.; Santaella, C.; Montisci, M. J.; Vierling, P.; Riess, J. G. *Biochim. Biophys. Acta* **1994**, *1194*, 61–68.
(23) Gadras, C.; Santaella, C.; Vierling, P. *J. Controlled Release* **1999**, *57*, 29–34.
(24) Rolland, J. P.; Santaella, C.; Vierling, P. *Chem. Phys. Lipids* **1996**, *79*, 71–77.
(25) Schlossman, M. L.; Synal, D.; Guan, Y. M.; Meron, M.; Shea-McCarthy, G.; Huang, Z. Q.; Acero, A.; Williams, S. M.; Rice, S. A.; Viccaro, P. J. *Rev. Sci. Instrum.* **1997**, *68*, 4372–4384.

the subphase, i.e., $Q_z = (4\pi/\lambda) \sin \varphi$ in which φ is the incident angle and λ is the wavelength). The monolayers were allowed to stand for 30 min, compressed to the desired pressure, and then allowed to equilibrate for another 10 min prior to data collection. Because of the intensity of the beam available from the undulator source, it was possible to measure absolute reflectivities as low as 10^{-9}, allowing for a large Q_z range and therefore a more reliable fit to the experimental data. Reflectivity profiles were collected at surface pressures of 0, 15, and 30 mN m^{-1} except for FDGL, which was recorded at 0, 10, and 20 mN m^{-1}.

Models were fitted to the experimental reflectivity profiles using the Motofit program.[26] The data were fitted to a layer model, in which the interface was modeled as a series of layers characterized by three parameters: layer thickness, scattering length density (SLD), and a Gaussian roughness between layers. Known values were used for the SLD of the subphase and air, and a fixed roughness of 3 Å was used for the air/film interface. It is always preferable to use the smallest number of layers that adequately fits the data, and in this work a two-layer fit gave good results in all cases.

Results and Discussion

Surface Pressure−Area Isotherms. To measure the surface properties of FDGL and FDGL-NTA-Ni monolayers, $\pi-A$ isotherms were recorded and compared with isotherms obtained for monolayers of two non-fluorinated lipids, DOPC and DOGS-NTA-Ni, in isolation and in a 1:1 mixed monolayer. The non-fluorinated lipids are commercially available and are commonly used for template-mediated crystallization and/or single particle analysis of membrane proteins.[18,20,27,28]

The $\pi-A$ isotherms obtained for DOPC and DOGS-NTA-Ni (Figure 2A) were similar to those reported previously.[29−31] The monolayers were stable up to surface pressures (π) of 42 and 41 mN m^{-1}, respectively. The isotherms exhibited a steady increase in π up to the point of collapse with no noticeable phase transitions, which is expected given the unsaturation present in the hydrocarbon tails of the lipids. The limiting molecular area of the non-fluorinated lipids agreed well with expected values;[29−31] however, for DOPC the collapse pressure was slightly lower than reported previously (π_c = 42 mN m^{-1} vs 47−49 mN m^{-1}).[30,31] Isotherms of the 1:1 mixed monolayer of DOPC and DOGS-NTA-Ni indicated that the molecular areas exhibit an additive behavior, indicating that the components either mix ideally or are totally immiscible.

Monolayers of the nickel-chelating functionalized lipid, FDGL-NTA-Ni, were stable up to a collapse point of π = 41 mN m^{-1}, and like the non-fluorinated lipids did not appear to undergo a phase transition. The diluent lipid, FDGL, exhibited different surface behavior. Surface pressure increased rapidly up to π = 22 mN m^{-1}, and a molecular area of 80 Å^2 at which point a plateau in the pressure profile was observed, which given the small molecular areas is likely to represent a collapse to a multilayered phase. Like the non-fluorinated lipids, the isotherm of the 1:1 mixed monolayer of the fluorinated lipids showed behavior and molecular areas that lay between those of the two pure components, again indicating that the fluorinated lipids mix ideally or not at all.

The fluid phase limiting molecular areas (Table 1, A_0) observed for the fluorinated lipids are larger than those observed for the corresponding non-fluorinated lipids (93 Å^2 vs 84 Å^2 for the diluent lipids, 85 Å^2 vs 74 Å^2 for the Ni-chelating lipids). This is not surprising given that the fluorinated lipids have four chains. The similarity of the limiting areas of the fluorinated molecules to that of the non-fluorinated ones suggests that close packing is enhanced in the fluorinated molecules. Furthermore, the slope of the fluid phase region of the fluorinated molecules indicates that, particularly for the Ni-chelating lipid, compressibility is higher than that of the non-fluorinated molecules, most likely as a result of the addition of the extra alkane chains.

Only limited data are available describing the surface behavior of fluorinated lipids similar to FDGL-NTA-Ni. Isotherms of a previously reported phosphate-linked lipid show the absence of any phase transitions, consistent with the lipid in this study, and indicated a collapse at 32 Å^2 and π = 45 mN m^{-1}.[17] The relatively large molecular area of the lipids evaluated in this study can be attributed to the more extensive branching of the hydrocarbon regions of FDGL-NTA-Ni and FDGL, introduced to enhance the fluidity of the monolayer. The data are therefore consistent with the design objectives having been met.

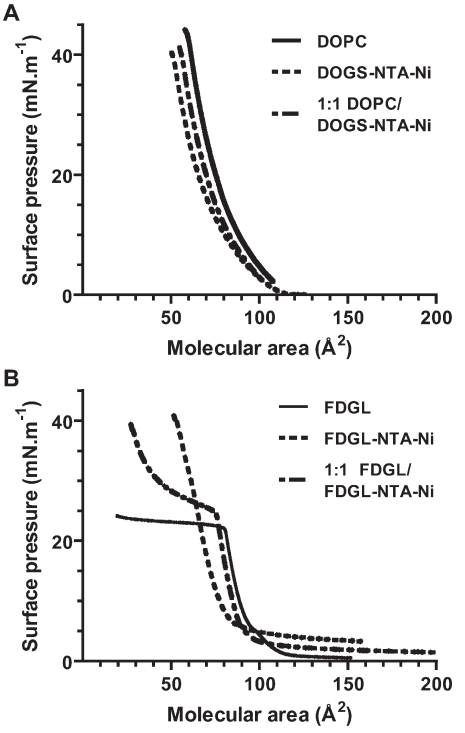

Figure 2. Surface pressure versus area isotherms for non-fluorinated and fluorinated lipid mixtures spread on a H_2O subphase. (A) DOPC (solid line), DOGS-NTA-Ni (dotted), and 1:1 mixture of the two non-fluorinated lipids (dot-dash). (B) FDGL (solid), FDGL-NTA-Ni (dotted), and a 1:1 mixture of the two fluorinated lipids (dot-dash).

Table 1. $\pi-A$ Isotherms of Partially Fluorinated and Non-fluorinated Lipids[a]

	A_0[b] (Å^2)	A_c[c] (Å^2)	π_c[c] (mN m^{-1})
FDGL	93 (0.3)	80 (1.1)	22 (0.1)
FDGL-NTA-Ni	85 (0.9)	52 (1.0)	41 (0.3)
1:1 FDGL/FDGL-NTA-Ni	89 (0.3)	73 (1.5)	25 (0.2)
DOPC	84 (1.7)	59 (1.4)	42 (2.0)
DOGS-NTA-Ni	74 (0.7)	51 (0.8)	41 (0.2)
1:1 DOPC/DOGS-NTA-Ni	76 (1.5)	55 (1.1)	41 (1.5)

[a] Standard errors are shown in parentheses. [b] A_0 = limiting molecular area. [c] A_c = area at collapse; π_c = surface pressure at collapse. The collapse point for FDGL and 1:1 FDGL/FDGL-NTA-Ni represents a collapse into a multilayered phase.

(26) Nelson, A. *J. Appl. Crystallogr.* **2006**, *39*, 273–276.
(27) Avila-Sakar, A. J.; Guan, T. L.; Arad, T.; Schmid, M. F.; Loke, T. W.; Yonath, A.; Piefke, J.; Franceschi, F.; Chiu, W. *J. Mol. Biol.* **1994**, *239*, 689–97.
(28) Hagnerelle, X.; Plisson, C.; Lambert, O.; Marco, S.; Rigaud, J. L.; Johannes, L.; Levy, D. *J. Struct. Biol.* **2002**, *139*, 113–121.
(29) Isarankura-Na-Ayudhya, C.; Prachayasittikul, V.; Galla, H. J. *Eur. Biophys. J.* **2004**, *33*, 522–534.
(30) Vie, V.; Van Mau, N.; Lesniewska, E.; Goudonnet, J. P.; Heitz, F.; Le Grimellec, C. *Langmuir* **1998**, *14*, 4574–4583.
(31) Yan, W. F.; Piknova, B.; Hall, S. B. *Biophys. J.* **2005**, *89*, 306–314.

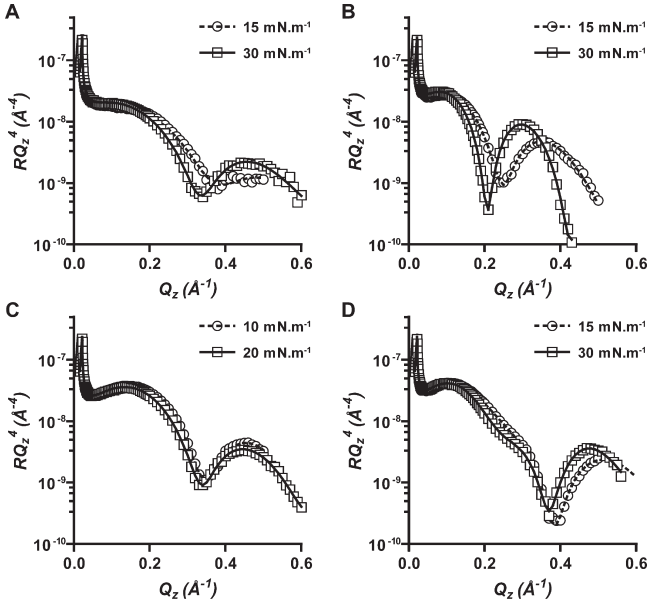

Figure 3. Reflectivity curves collected from Langmuir monolayers of DOPC (A), DOGS-NTA-Ni (B), FDGL (C), and FDGL-NTA-Ni (D). Monolayers were spread on a H_2O subphase and compressed to either 15 mN m^{-1} (open circles) or 30 mN m^{-1} (open squares) prior to data collection in all cases, except for FDGL which was compressed to 10 mN m^{-1} (open circles) or 20 mN m^{-1} (open squares). The reflectivity profiles are displayed as RQ_z^4 vs Q_z to remove the contribution of the Fresnel reflectivity. Fits to the data are shown as dotted or solid lines for the low- and high-pressure measurements, respectively, and demonstrate the quality of fit, validating the models shown in Figure 4.

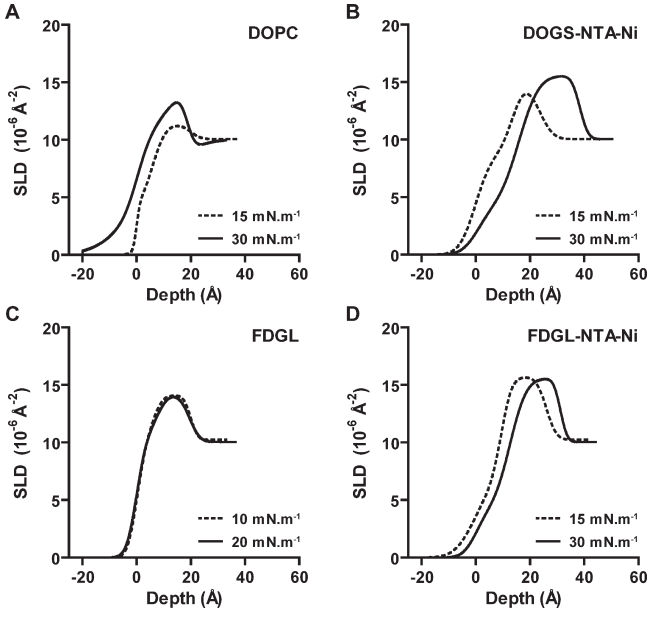

Figure 4. Two-component electron density profiles modeled from the fitted data displayed in Figure 3. Models for DOPC (A), DOGS-NTA-Ni (B), FDGL (C), and FDGL-NTA-Ni (D) are represented graphically as scattering length density (SLD) versus depth from the air−water interface. Electron density profiles shown are modeled to data recorded at high (solid line) and low pressure (dashed line).

X-ray Reflectometry. To investigate the packing density of the fluorinated and non-fluorinated lipids described above, X-ray reflectivity profiles (Figure 3) were recorded and analyzed (Figure 4) for each of the pure lipid monolayer systems shown in Figure 1. The reflectivity profiles were analyzed by modeling the data as a two-layer system (Figure 4, Table 2). Molecular dimensions estimated from simple models of the fluorinated lipids in an extended conformation were then used to interpret the measurements obtained from modeling of the reflectivity data. For the non-fluorinated lipids, we rationalized that layer 1 represented the hydrocarbon tails, while layer 2 incorporates the diglyceride linker and the phosphocholine or Ni-NTA headgroup (Figure 5A). At low surface pressures the layer boundary was shifted closer to the aliphatic end of the lipid. The observed overall increase in the combined layer thickness of the DOGS-NTA-Ni system, particularly considered relative to the change in the DOPC system, may indicate that the headgroup adopts a more extended conformation as the system becomes more crowded.

Table 2. Reflectometry Results Obtained by Modeling Data for Langmuir Films of Partially Fluorinated and Non-fluorinated Lipids[a]

	pressure (mN m^{-1})	layer	thickness (Å)	SLD ($\times 10^{-6}$ Å^{-2})	interfacial roughness (Å)
FDGL	10	1	6.0	9.8	2.7
		2	13.9	14.1	2.9
	20	1	7.9	10.8	3.0
		2	11.7	14.1	3.0
FDGL-NTA-Ni	15	1	9.6	7.1	6.0
		2	16.4	15.7	3.0
	30	1	12.6	4.1	3.9
		2	18.6	15.6	4.8
DOPC	15	1	5.7	3.9	1.0
		2	14.3	11.3	3.9
	30	1	9.3	6.7	3.3
		2	9.6	12.8	2.8
DOGS-NTA-Ni	15	1	13.6	8.9	4.7
		2	9.7	15.1	3.6
	30	1	20.6	9.9	4.3
		2	8.7	16.4	8.8

[a] Estimated uncertainty of the models is ±10%.

In the case of the fluorinated lipids, we rationalized that layer 1 describes the behavior of the branched hydrocarbon tails only, while layer 2 incorporates the fluorocarbon core and the hydrophilic headgroup (Figure 5B). Layer 1 undergoes an increase in thickness for both fluorinated lipids as the surface pressure increases. This is best explained by a conformational change in the lipid tails to a more extended state (allowing more condensed packing) as the monolayer is compressed.

The difference in the combined thickness of layer 2 between FDGL and FDGL-NTA-Ni was approximately 3−6 Å. Although this was difficult to measure accurately due to differences in the isotherm pressures, the data suggest that the linker coupled to the Ni-NTA headgroup (estimated to be 12 Å in a fully extended conformation) does not fully extend into the aqueous subphase. This is likely due to the flexibility of the functionalized headgroup but may alternatively suggest a weak interaction between the Ni-NTA and adjacent lipids in the monolayer.

In all the lipid systems tested, layer 2 had a higher scattering length density than layer 1. For the non-fluorinated materials this would be the result of the fact that the head groups and included water in layer 2 contribute more electrons than the atoms in layer 1. In the case of the non-fluorinated molecules, there are four chains per molecule contributing to layer 1, but only two chains in layer 2. The contribution of the electrons from the fluorine atoms is more than enough to compensate for this, however, and it is therefore expected that the fluorinated region should have a higher SLD. Perhaps surprisingly, however, the SLD values of the layers for both the fluorinated lipids and the non-fluorinated counterparts were very similar, despite the fluorine atoms and the

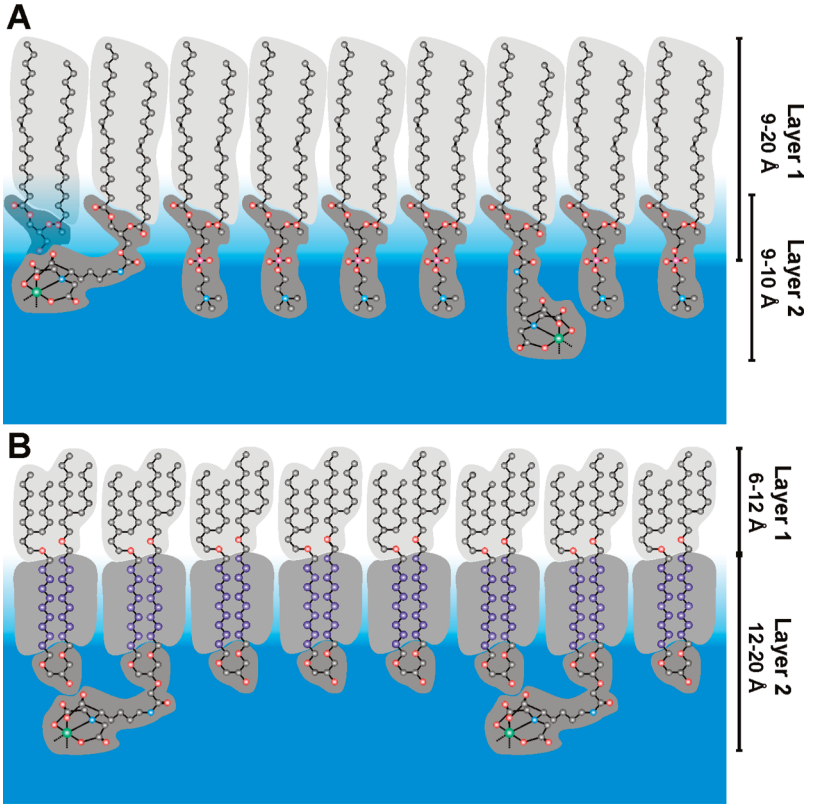

Figure 5. Schematic representation of the predicted packing behavior of mixed monolayers of the non-fluorinated (A) and fluorinated lipids (B) characterized in this study. Dimensions of the two layers resolved by X-ray reflectometry are indicated on the right. The overlap in the layer dimensions of the non-fluorinated lipids reflects the observed shift of the layer boundary between the data recorded at low and high surface pressure. The molecular dimensions of the fluorinated lipids suggest that the Ni-NTA headgroup of the functionalized lipid does not fully extend into the aqueous subphase.

fact that the fluorinated lipids are more highly branched at the ends of the hydrocarbon chains. For that reason, it is likely that the average number density of the chains in layer 2 in the fluorinated lipids is lower than that in the non-fluorinated materials. This is somewhat surprising, as preliminary studies [Landsberg, M.; Hussein, W., et al., unpublished data] suggest that incorporation of fluorinated lipids into the monolayer approximately doubles the time that supported monolayers are stable in the presence of disruptive concentrations of detergents, relative to monolayers prepared from commercially available hydrocarbon-based lipids.[32] It may have been expected that this behavior could be a result of tightly packed fluorocarbon domains leading to increased stability. Our results suggest that this is not the case, although because the scattering length densities are averaged over the entire film, the existence of lateral structure in the form of close-packed fluorinated domains coexisting with more fluid regions is not precluded. We therefore expect that the increased stability is likely a result of fundamental incompatibility between the fluorocarbon region of the lipids and the detergent causing phase separation which is far less likely to occur in the non-fluorinated case. The branched hydrocarbon tails incorporated into the fluorinated lipids appear to impart sufficient fluidity to the mixed monolayer to allow lateral diffusion and subsequent 2D array formation of proteins tethered by the lipid headgroup at the air−water interface,[16] consistent with the observation here that in pure monolayers of the fluorinated lipids the compressibility was higher than that of the non-fluorinated materials.

(32) Kelly, D. F.; Abeyrathne, P. D.; Dukovski, D.; Walz, T. *J. Mol. Biol.* **2008**, *382*, 423–433.

Conclusions

The use of fluorinated lipids as monolayer-forming templates for protein crystallization was first reported over 10 years ago.[11] An innovative approach to obtaining 2D crystals of retinoid receptors required the synthesis of a partially fluorinated lipid conjugated to retinoic acid. The hydrophobic retinoid ligand conjugated to the lipid head exhibited a tendency to bury itself in the alkyl chain region of non-fluorinated lipid analogues when spread into monolayers at the air−water interface. Substituting parts of the hydrocarbon chain for fluorocarbons, however, excluded the hydrophobic ligand from the fluorinated monolayer film, making it available for binding to the retinoid receptor in the aqueous subphase.[11] Subsequent to this, the possibility that fluorinated lipids may be ideal candidates for the development of monolayer-forming lipids resistant to destabilization by a broad range of detergents and amphipathic molecules is an area that has attracted significant interest in membrane protein structural biology.

Studied in comparison to a selection of commercially available lipids commonly used for template-assisted crystallization of macromolecules, the fluorinated lipids evaluated in this study exhibit a number of properties which suggest they will be of value for the 2D crystallization of detergent-solubilized, His-tagged membrane proteins. FDGL and FDGL-NTA-Ni both spread into stable, fluid monolayers at the air−water interface. The fluorinated lipids have a larger average cross-sectional area but are more compressible and collapse at lower pressures than the non-fluorinated lipids. X-ray reflectivity analyses are able to resolve two regions within the fluorinated lipid monolayers with distinguishable electron density profiles: an electron dense region

consisting of the fluorocarbon film and the lipid headgroup and a slightly less electron dense region encompassing the branched hydrocarbon chains. Given the higher electron density of fluorine, the closeness of these two measurements suggests that the fluorinated layer is less dense and therefore less tightly packed. This in turn suggests that the enhanced stability and reduced permeability of partially fluorinated lipid molecules may be attributable to the formation of a perfluorinated film (Figure 5B) which is fundamentally incompatible with and therefore less prone to the destabilizing effects of detergents, when compared with traditional, non-fluorinated lipid monolayer systems. Additionally, the X-ray reflectivity data suggest that the Ni-NTA group incorporated into the head of the FDGL-NTA-Ni lipid may not fully extend into the aqueous phase. To this end, future synthetic targets may include lipids with alternative headgroup structures to ensure optimal presentation of the functional group in the aqueous subphase and thus maximum availability of the Ni-NTA ligand for binding by His-tagged proteins in 2D crystallization studies.

Acknowledgment. The assistance of Drs. Binhua Lin and Mati Meron of the Consortium of Advanced Radiation Sources with setup and software for reflectometry work is gratefully acknowledged. Reflectometry experiments were performed at the Advanced Photon Source with support from the Australian Synchrotron Research Program, which is funded by the Commonwealth of Australia under the Major National Research Facilities Program. Use of the Advanced Photon Source was supported by the U.S. Department of Energy, Office of Science, Office of Basic Energy Sciences, under Contract No. W-31-109-Eng-38. This work was also supported in part by an Australian Research Council Project Grant to B.H. and R.P.M. (DP0556547).